

Supplementary Material (ESI) for *PCCP*  
This journal is © the Owner Societies 2010

### An improved method to measure the rate of evaporation and thermal decomposition of high boiling organic and ionic liquids by thermogravimetical analysis

Florian Heym<sup>a</sup>, Bastian J. M. Etzold<sup>b</sup>, Christoph Kern<sup>a</sup>, Andreas Jess<sup>a</sup>

<sup>a</sup> Chair of Chemical Engineering, University Bayreuth, D-95440 Bayreuth, Germany, Jess@uni-bayreuth.de

<sup>b</sup> Chair of Chemical Reaction Engineering, University Erlangen-Nuremberg, D-91058 Erlangen, Germany

## Electronic Supplementary Information

### Finite element simulation

To derive the correlation (Eq. 18) for the mass transfer coefficient of cylindrical crucibles in overflow of an inert gas, numerical calculations were carried out with the software Comsol Multiphysics 3.5a. Fig. 13 shows a scheme of the set up within the finite element software.

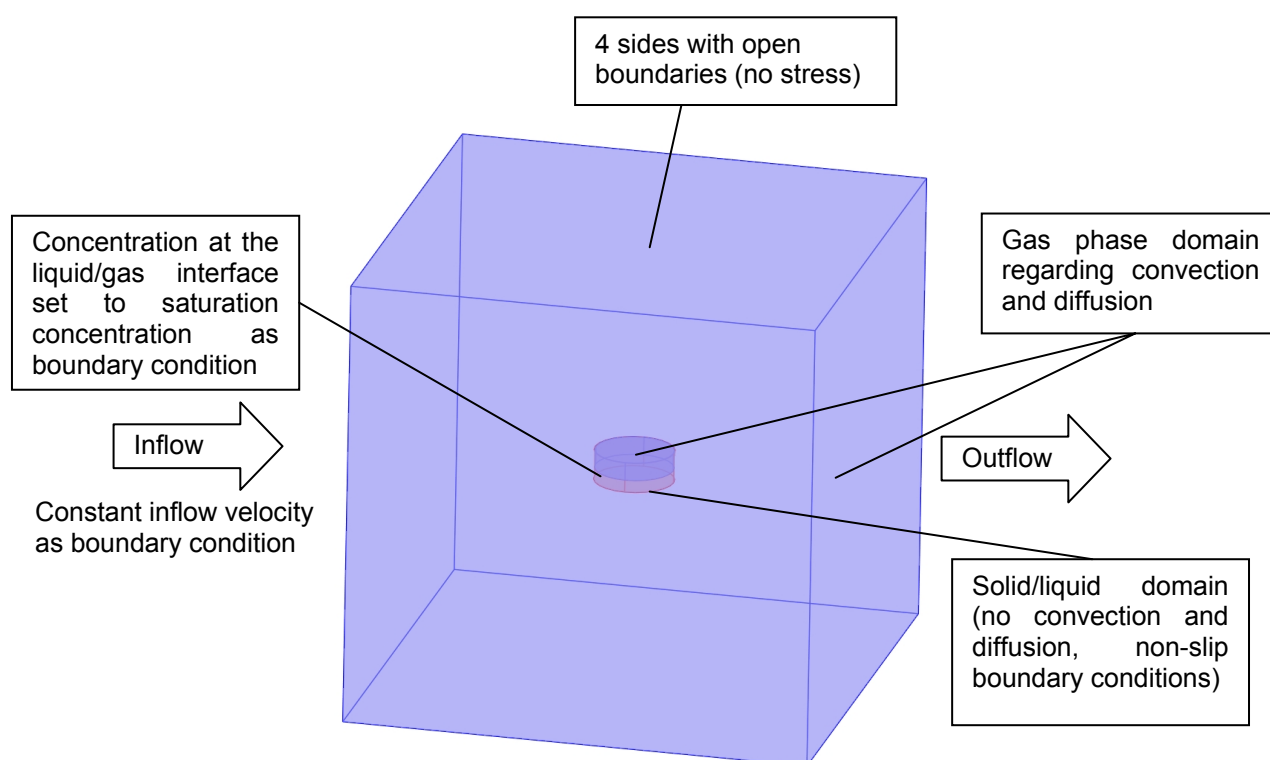


**Fig. 13:** Scheme of the simulated finite element problem of a TG crucible (overflow of gas)

The geometries of 6 crucibles representing a broad range of diameter-to-height ratios were implemented (Tab 3). The temperature was set to 340 °C. Most simulations were carried out with N<sub>2</sub> ( $\rho = 0.556 \text{ kg m}^{-3}$ ,  $\nu = 5.4 \cdot 10^{-5} \text{ m}^2 \text{ s}^{-1}$ ); the diffusion coefficient of [BMIM] [BTA] calculated by Eq. (17) was used ( $D = 1.7 \cdot 10^{-5} \text{ m}^2 \text{ s}^{-1}$ ) and the vapour pressure set to 37 Pa. As for finite element methods the mesh generation has major influence on the accuracy of the results, differently coarse and fine meshes were tested and compared. For the mesh generation a finer mesh was created at the boundary regions, where high gradients occur.

A mesh with approx. 60,000 elements showed only minor error (< 2%) compared to finer meshes. Fig. 14 shows a top view of a representative mesh.

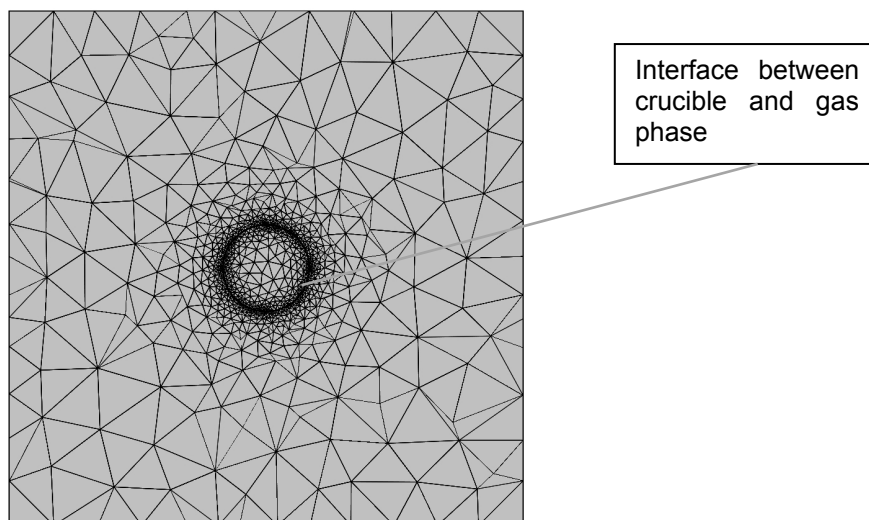


**Fig. 14:** Representative mesh used for the generation of the finite elements

The main parameters varied within the simulations are listed in Tab. 3 and are the crucible geometries, the filling level and the inlet velocity of the gas.

**Tab. 3:** Simulation parameters for calculations performed with N<sub>2</sub> as purge gas

Crucible no.	d <sub>C,outer</sub> in mm	d <sub>C,inner</sub> in mm	h <sub>C</sub> in mm	u in m s <sup>-1</sup>	h <sub>F</sub> in mm
1	10.2	10	2	0, 0.005, 0.01, 0.1, 1	0.05, 0.4, 0.8, 1.2, 1.6, 1.8, 2
2	5.1	5	2	0, 0.005, 0.01, 0.1, 1	0.05, 0.8, 2
3	2.55	2.45	2	0, 0.005, 0.01, 0.1, 1	0.05, 0.8, 2
4	1.275	1.175	2	0, 0.005, 0.01, 0.1, 1	0.05, 0.8, 2
5	2.55	2.45	0.5	0, 0.005, 0.01, 0.1, 1	0.0125, 0.2, 5
6	1.275	1.178	0.5	0	0.0125, 0.2, 5

The steady state simulation was evaluated by integration of the molar stream  $\dot{n}_{evap}$  leaving the crucible. From the given evaporation surface and saturation concentration the mass transfer coefficient  $\beta$  and the Sh number were calculated:

$$\beta = \frac{\dot{n}_{evap}}{A_{evap} \cdot c_{sat}} = \frac{\dot{n}_{evap} \cdot R \cdot T}{A_{evap} \cdot p_{vap}}, Sh = \frac{\beta \cdot d_C}{D} \quad (28)$$

Prior to deriving the correlation (18) the influence of the vapour pressure and the purge gas was checked. For the crucible no. 2 (Tab. 3), a filling level of 0.8 mm and inlet velocities as given in Tab. 3 the vapour pressure was varied (1, 25, 37, 50, 100, 500, 10000 Pa). As expected no influence of the vapour pressure on the resulting mass transfer coefficient was seen. Secondly, simulations with He ( $\rho = 0.080 \text{ kg m}^{-3}$ ,  $\nu = 4.1 \cdot 10^{-5} \text{ m}^2 \text{ s}^{-1}$ ,  $D = 5.8 \cdot 10^{-5} \text{ m}^2 \text{ s}^{-1}$ ) were performed for the crucible geometry 2, three filling levels (0.05, 0.8, 2 mm) and the inlet

velocities given in Tab. 3. To show that the gas type has no influence on the simulation data, the obtained Sh numbers from N<sub>2</sub> and He are plotted in Fig. 15 versus  $Re_d^{0.5} Sc^{1/3}$ . Clearly, the results lie within a minor numerical error on straight lines for a given filling height.

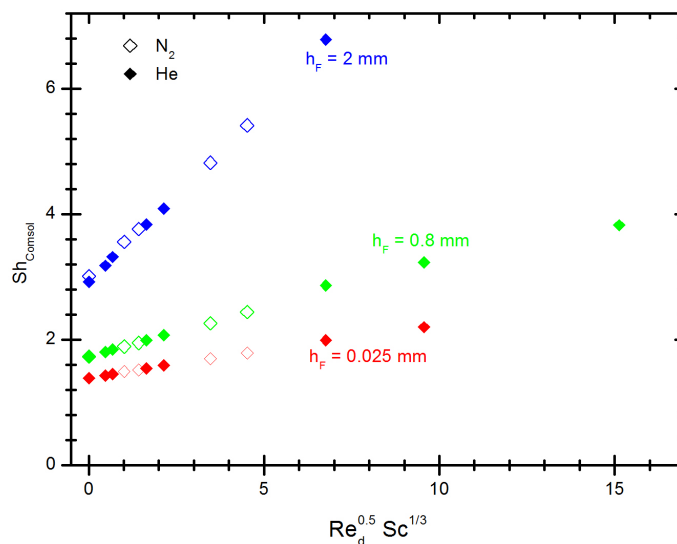


**Fig. 15:** Comparison of Sh numbers obtained for N<sub>2</sub> and He as purging gas

The Sh correlation (Eq. (18)) was finally obtained by minimizing the following error sum of squares (ESS) over all simulations given in Tab. 3 and the simulations with He as purge gas. The numbers 2.9 and 0.58 in Eq. (18b) represent the fitting parameters:

$$ESS = \sum_{\text{all simulations}} \left( \frac{Sh_{correlation} - Sh_{simulation}}{Sh_{correlation}} \right)^2 \quad (29)$$

The parity plot given in Fig. 16 shows a good agreement of the Sh numbers obtained by the correlation and the simulations.

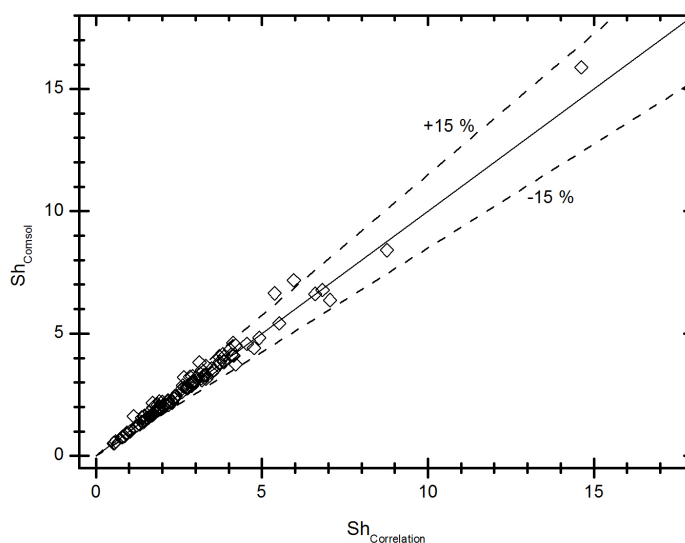


**Fig. 16** Parity plot comparing the Sh numbers obtained by the simulation and after the derived correlation.

### **Videos showing the concentration and velocity profiles**

The supplementary information contains also two videos (norm\_conc\_d=5.1\_h=2.mov and norm\_vel\_d=5.1\_h=2.mov). They show the concentration and velocity profile calculated for the crucible geometry no. 2 (Tab. 3) with N<sub>2</sub> as overflowing gas. The filling height  $h_F$  is 0.8 mm and the videos show the respective situations for different gas inlet velocities in the range of  $1 \cdot 10^{-4}$  to  $1 \text{ m s}^{-1}$ . The videos show the steady state solutions starting with the lowest velocity one after another (the actual inlet velocity  $u_0$  is indicated by the title). For clearness, the concentration is normalized to the saturation concentration and the velocity to the mean inlet velocity.